# Visible-Wavelength Spectroscopy of Asteroids

**Article** · January 2002

**3 authors:**

Schelte J. Bus
University of Hawaiʻi at Mānoa
**1,624** PUBLICATIONS **7,823** CITATIONS

SEE PROFILE

Faith Vilas
Planetary Science Institute
**410** PUBLICATIONS **4,594** CITATIONS

SEE PROFILE

Maria Antonietta Barucci
Observatoire de Paris
**633** PUBLICATIONS **15,560** CITATIONS

SEE PROFILE

**Some of the authors of this publication are also working on these related projects:**

Differentiation in the outer belt View project

UV-VIS spectrophotometry and polarimetry of near-perihelion sublimation activity of main-belt primitive asteroids View project

# Visible-Wavelength Spectroscopy of Asteroids

**Schelte J. Bus**
*University of Hawai'i*

**Faith Vilas**
*NASA Johnson Space Center*

**M. Antonietta Barucci**
*Observatoire de Paris–Meudon*

Since first becoming available for astronomical research in the early 1980s, charge-coupled-device (CCD) spectrographs have had a profound impact on our ability to measure the spectral-reflectance properties of asteroids. High signal-to-noise, low-resolution spectra, covering the visible-wavelength region from 0.4 to 1.0 μm, are now routinely obtained for asteroids much fainter than were measured during the Eight-Color Asteroid Survey. By recording the entire spectral range in a single exposure, some of the difficulties associated with multifilter photometry, arising from the inherent rotation of asteroids or from temporal variations in sky conditions, can be avoided. Studies involving CCD spectroscopy have resulted in the discovery of several absorption features in the spectra of asteroids and have provided new insights into the compositional nature of asteroid surfaces. Spectral surveys have also helped to refine our understanding of the orbital distributions of asteroid classes. We discuss the practical aspects of asteroid spectroscopy, focusing on observing procedures, data reduction techniques, and potential sources for uncertainty in the reduced spectra. We also review some of the applications of asteroid spectroscopy, and discuss how these observations have impacted the structure of asteroid taxonomy.

## 1. INTRODUCTION

A fundamental characteristic of an asteroid is its color. Incidental sunlight is either scattered or absorbed by mineral grains on an asteroid's surface; depending on the optical properties of these grains, the fraction of light that is reflected to Earth can vary as a function of wavelength. Based on his microphotometric measurements of photographic spectra, *Bobrovnikoff* (1929) first reported variations in the color of asteroids. Bobrovnikoff noted differences in the spectral continua of 12 asteroids, measured over the wavelength interval of 0.39–0.47 μm, and even monitored changes in the color of Vesta over time, which he was able to correlate with the asteroid's rotation. However, because of the limitations of photographic spectroscopy, very little progress was made in the study of asteroid colors until the advent of photoelectric detectors. A systematic investigation of the broadband UBV colors of asteroids was begun in the mid-1950s, leading to the identification of two distinct populations of objects based on their spectral reflectance properties (*Wood and Kuiper,* 1963).

The true spectral nature of asteroids started to become apparent as programs of narrow-band spectrophotometry were initiated in the late 1960s (*McCord et al.,* 1970; *Chapman et al.,* 1971). These narrow-band observations sampled the entire visible spectrum, from 0.3 to 1.1 μm, with higher spectral resolution than before. Besides the diversity in color that was observed, these data helped define some of the key characteristics that describe asteroid spectra over the visible spectrum, including strong absorption bands in the UV and near 1 μm (e.g., *Chapman and Gaffey,* 1979). These data also provided the basis for developing the first rigorous asteroid taxonomy (*Chapman et al.,* 1975) and allowed for more thorough characterizations of asteroid surface materials in the context of mineralogy (e.g., *Gaffey and McCord,* 1979).

Spectrophotometric studies of asteroids peaked in the mid-1980s with the completion of the Eight-Color Asteroid Survey (ECAS) (*Zellner et al.,* 1985). Using specially chosen filters with bandpasses targeting the major features contained in asteroid spectra, this survey sampled nearly 600 asteroids and formed the basis for the Tholen taxonomy (*Tholen,* 1984). At about the same time, a new generation of astronomical spectrographs was being developed that incorporated charge-coupled-device (CCD) cameras to record the spectra. Originally designed as an electronic analog to magnetic bubble memory, the introduction of CCDs as optical detectors helped revolutionize many areas of observational astronomy (*Janesick and Elliott,* 1992). The high sensitivity and stable, two-dimensional format of a CCD makes it ideal for use in spectroscopy. The use of long-slit spectrographs in the study of asteroids has many advantages over traditional filter photometry. These spectrographs provide the capability of imaging much, if not all, of the visible spectrum in a single exposure, with spectral resolutions that are much higher than possible with standard photometry. This essentially eliminates the potential for uncertain-

ties that can arise due to photometric variability tied to an asteroid's rotation. Along with the asteroid spectrum, the background sky is measured simultaneously along the spectrograph slit, allowing for much more precise fitting and removal of the sky than was ever before possible. Unlike spectrophotometry, which demands that measurements be made under clear skies, spectroscopy does not require photometric conditions, and thus a larger fraction of the available telescope time can be utilized.

The primary objective in reflectance spectroscopy is simple: to determine the ratio of reflected sunlight to incident sunlight as a function of wavelength. There are several factors, however, that add to the complexity of asteroid spectroscopy and contribute to uncertainties in the observations. First, the fact that the Sun cannot be directly measured with a CCD spectrograph requires the use of other solar-like stars that act as spectral proxies. Any differences between the spectra of these solar analogs and the actual solar spectrum can result in artifacts in the reduced asteroid spectrum. Because the sunlight reflected from an asteroid only interacts with grains on the very top surface, the measured spectrum represents only the optical properties of those grains. It is generally assumed that this upper surface material is representative of the bulk composition of the asteroid, but other properties of these grains, including their temperature, size distribution, and the effects of long-term exposure to space, can also affect their spectral properties. Since the disks of asteroids are unresolved as viewed from Earth, the measured spectrum represents the reflectance characteristics averaged over the entire illuminated disk and can be affected by changes in viewing geometry. Before the light reflected from the asteroid reaches Earth's surface, it passes through our atmosphere, where it can be scattered and absorbed. Some of the most difficult aspects of reducing asteroid spectra involve correcting for these atmospheric effects. Finally, the characteristics of both the spectrograph and detector must be understood, so that any instrumental offsets that might be present in the measurements can be calibrated and removed.

## 2.  INSTRUMENTATION

A CCD is a two-dimensional, solid-state detector that is sensitive to visible-wavelength light. It is composed of an array of closely spaced capacitors, commonly referred to as picture elements or pixels. When a positive potential is placed across this array, a potential well is formed at the location of each pixel. These potential wells collect and hold electrons that are freed when incoming photons interact with the silicon atoms that make up the detector substrate. At the completion of an exposure, the collected charge is read out by manipulating the voltages between the rows and columns of the array in a systematic way, stepping the charge across the detector pixel by pixel. The output signal is then amplified and converted into counts, or analog-digital units (ADUs), to make up the resulting image.

The advantages of CCDs over older two-dimensional detectors are numerous. They are dimensionally very stable and typically have high sensitivities (quantum efficiencies or "QE") over the visible wavelengths; they also typically have low read noise and a large, linear dynamic range. While the use of CCDs in astronomical imaging evolved rapidly in the mid- to late 1970s, the widespread application of CCDs to astronomical spectroscopy did not occur for nearly a decade. This delay can mainly be attributed to the time required for the design and fabrication of new long-slit spectrographs that could take full advantage of the sensitivity and large format offered by CCDs.

Long-slit CCD spectrographs are capable of low- to medium-resolution spectroscopy (R ~ 100–5000, where R is defined as $\lambda/d\lambda$) while recording spatial detail along a one-dimensional cut on the sky defined by the length and orientation of the spectrograph slit. For asteroids, this long-slit capability means that a sample of the surrounding sky is measured simultaneously with the asteroid, as shown in Fig. 1a, allowing for a much more precise determination and removal of the background sky signal. To obtain the highest possible signal-to-noise (S/N) spectra for faint asteroids, observations are usually made at very low spectral resolutions, so that the flux from an asteroid is spread over the fewest number of pixels along the dispersion direction. This low spectral resolution can be achieved with spectrographs utilizing either reflection gratings or grisms (a combined grating and prism) as the dispersing element. Grism spectrographs are particularly powerful in that they are capable of imaging the entire visible spectrum in one exposure, although the proper selection and use of blocking filters is necessary to avoid the overlap of spectral orders (*Xu et al.,* 1995). The total wavelength coverage that can be achieved with any spectrograph depends strongly on the throughput of its optics and the QE of the CCD. Though some systems have been optimized for observations in the UV (e.g., *Cochran and Vilas,* 1997), the sensitivity of many CCD spectrographs falls off sharply short of 0.4 μm, such that the resulting asteroid spectra do not extend as far into the UV as those measured by filter photometry.

## 3.  OBSERVATIONS AND DATA REDUCTION

The observing strategies used in asteroid spectroscopy will vary depending on the telescope and instrumentation used and the goals of the particular observing program. In general, a sequence of observations includes several spectral images of the target asteroid and of one or more solar analog stars (*Hardorp,* 1978). Also, a series of calibration images are taken that include bias frames, flatfield images, and an arc lamp image for wavelength calibration.

Each asteroid and standard star observation is made by centering the object at a prescribed location along the slit, so that the maximum amount of light from the object passes through the slit. Because asteroids are typically moving against the background sky, offset rates are applied to the nominal sidereal track rate of the telescope (if possible) to improve the guiding. Many spectrographs are equipped with cameras that view the slit plane, allowing the sky region immediately outside the slit to be continuously monitored.
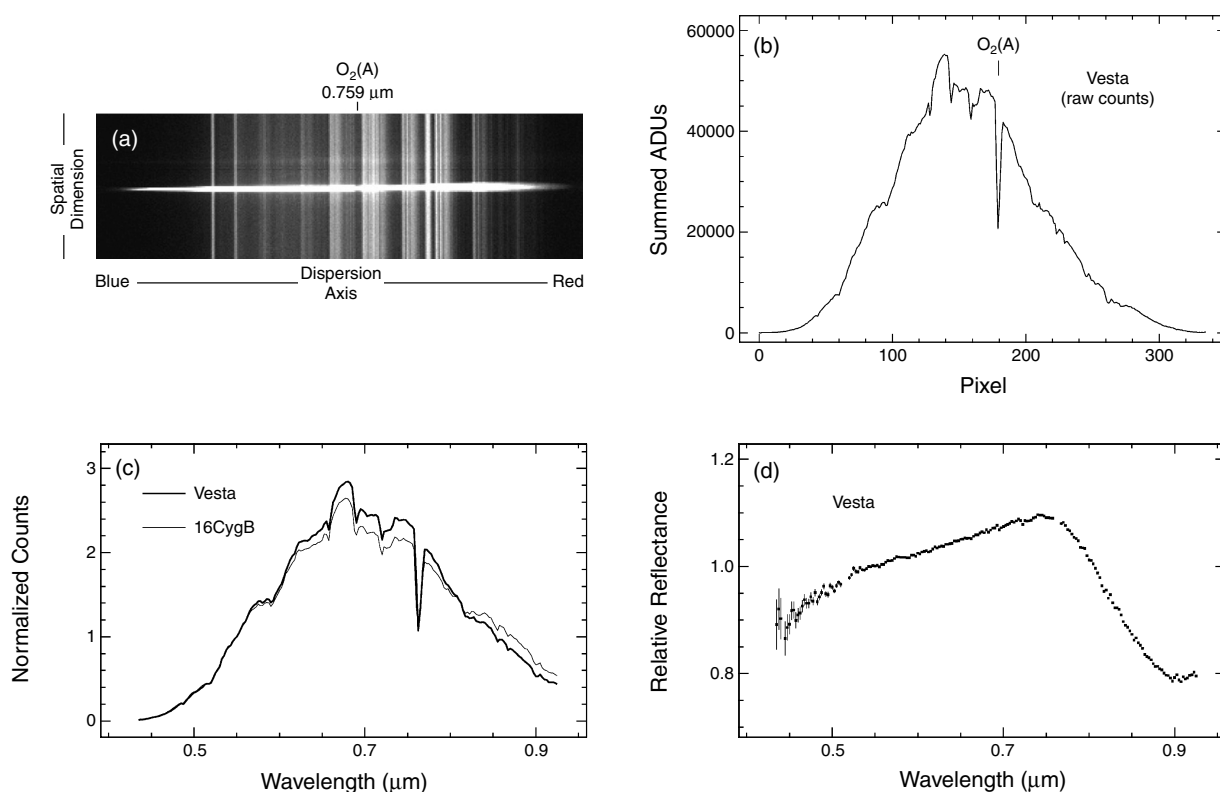
**Fig. 1.** Four steps in the reduction of asteroid spectra. **(a)** Spectral image of Vesta, taken on April 18, 1996, at the Michigan-Dartmouth-MIT Observatory, which has been bias and flat-field corrected. Bright vertical stripes (along the spatial dimension) are night-sky emission lines. The strong $O_2(A)$ atmospheric absorption band is labeled. **(b)** Extracted one-dimensional spectrum obtained by summing the object counts (ADUs) along each column within the extraction aperture and subtracting the fitted sky level. The falloff in sensitivity at both ends of the spectrum is clearly seen. **(c)** Spectrum for both Vesta and the solar-analog star 16CygB after each has been calibrated for dispersion (wavelength correction) and atmospheric extinction. To simplify the comparison, the counts in both spectra have been normalized to 1.0 at 0.55 μm. **(d)** Ratio spectrum (Vesta divided by solar analog), normalized at 0.55 μm. The formal error bars are very small except at the blue end of the spectrum.

By watching for spillover of the asteroid image outside the slit during an exposure, small corrections to the guiding can be made. Exposure times for the faintest targets are usually limited to 10–20 min, because of the accumulation of cosmic-ray events on the detector. Taking several images of each target asteroid and solar analog is always advisable. Besides helping to improve the overall S/N, multiple images allow for more complete identification and correction of discrepant pixels in the individual images and for the monitoring of any systematic offsets in the extracted spectra.

Bias frames are taken by setting the exposure to 0 s and keeping the shutter closed. The result is a readout of the bias level, the positive offset in the mean signal level of an image that results from the bias voltage applied across the CCD during each exposure. These bias images are used to create a residual bias structure frame that contains any low spatial-frequency variations in the bias level that might exist across the CCD. Flatfield images are taken to map the wavelength-dependent pixel-to-pixel variations in sensitivity across the CCD. These images are obtained by uniformly illuminating the spectrograph slit with a light source whose color closely approximates that of the nighttime sky. In spectroscopy, the flatfield correction accounts not only for variations in sensitivity across the CCD but also for spatial variations in the throughput of the spectrograph slit and optics.

The procedures for reducing and calibrating CCD spectra of asteroids were first outlined by *Vilas and Smith* (1985). Similar descriptions of the reduction process are given by *Luu and Jewitt* (1990), *Sawyer* (1991), *Xu et al.* (1995), *Bus and Binzel* (2002a), and others. Though the details may vary depending on the instrumentation and observing strategies used by each observing program, the fundamental steps used to reduce asteroid spectra remain the same. These steps can be summarized as four basic procedures:

1. *Preprocessing of the CCD images.* This involves the calibration and correction of systematic effects associated with the instrument and detector. Two principal corrections are included: the subtraction of a bias level followed by the division of a flat field. Secondary corrections may include subtraction of a dark current and identification and removal of cosmic-ray events. Correcting for the bias offset is usually done by first subtracting an average bias level derived from an overscan region contained in each image and then subtracting the residual structure frame.

A nightly flatfield image is created by averaging the individual flatfield frames taken throughout the night. This average flat is often fitted and ratioed to a high-order, two-dimensional surface, resulting in a flatfield image with an average value along the dispersion axis of ~1.0. When this normalized flat is then divided into each spectral image, small pixel-to-pixel variations in sensitivity are corrected without significantly changing the level of counts (ADUs) in the data. In very low-resolution spectroscopy, where spectra covering the entire sensitivity range of the detector are recorded in a single exposure, division by a flat field can sometimes lead to increased noise at the ends of the spectra. In this case, the flatfield correction is often omitted, and all object spectra are carefully positioned to lie on the same rows of the CCD. This allows for much of the variation in pixel-to-pixel sensitivity along the asteroid spectrum to be divided out in the ratio to the solar-analog spectrum.

2. *Extraction of one-dimensional spectra.* The spatial information contained in the two-dimensional image is collapsed to form a one-dimensional spectrum. First, a line is fitted that traces the peak flux along the length of the two-dimensional spectral image. Centered along this trace, an aperture is defined that has a fixed width and whose length contains the entire object spectrum. The width of this aperture is carefully chosen to contain most of the object flux while minimizing the amount of background sky that is included. Along each column of the image, the sky level is fitted and subtracted. The remaining object flux contained within the aperture is then summed along each column. The resulting spectrum represents the sky-subtracted counts of the object in ADUs as a function of row number, as shown in Fig. 1b.

3. *Calibration of the extracted spectra.* Wavelength and extinction corrections are now applied to each extracted spectrum. The wavelength, or dispersion correction is determined by measuring the column pixel positions for spectral lines recorded in the arc lamp image and fitting these to their known wavelength values. In applying the dispersion correction, the object spectrum is resampled, so that the channels of the corrected spectrum are uniformly spaced in wavelength, as shown in Fig. 1c. It is important that the flux is correctly partitioned between the new spectral channels, and that the total flux in the spectrum is conserved during this resampling.

A correction for atmospheric extinction is needed since the observations of asteroids and standard stars are typically obtained through different airmasses. Atmospheric extinction arises from a combination of Rayleigh scattering, ozone absorption, and extinction due to aerosols, and it is strongest at short wavelengths (*Hayes and Latham,* 1975). A nightly extinction model, giving extinction per airmass as a function of wavelength (spectral channel), can be created if observations of standard stars are obtained at several different airmasses throughout the night. Because extinction can vary with direction in the sky, calibration stars must also be observed over a range in azimuth. The calculated extinction coefficients are then used to correct the flux in each channel of the standard star spectrum to match the airmass of the asteroid observation (*Vilas and Smith,* 1985). A simpler though somewhat less precise approach to correcting for atmospheric extinction involves the use of mean extinction coefficients that have been previously measured for the observing site. The use of mean extinction coefficients works well if the observations of both the asteroids and standard stars are restricted to relatively low airmasses (*Bus,* 1999).

4. *Normalization to a solar-analog star.* The calibrated asteroid spectrum is finally divided by that of a standard solar-analog star. To facilitate the comparison of spectra for different objects, the ratioed asteroid spectrum is then normalized to unity at a standard wavelength, usually 0.55 μm (the center of the photometric V band) as shown in Figs. 1c and 1d or 0.70 μm (corresponding to the R band). An uncertainty for each channel can be calculated based on the gain and readnoise of the CCD, and the object and sky counts for both the asteroid and standard star spectra assuming Poisson statistics.

Residual features that do not divide out fully may be present in the normalized spectrum. These artifacts usually arise from temporal variations in the depths of atmospheric absorption bands or from the misalignment of stellar absorption lines due to small errors in the wavelength calibration. The latter is usually caused by instrument flexure or variations in the positioning of objects in the slit and can be minimized by applying small pixel shifts between the asteroid and solar analog spectra. For observations obtained using a wide slit, changes in seeing will alter the effective spectral resolution, resulting in a potential mismatch in line widths between the asteroid and solar analog spectra and leading to residual stellar line features in the normalized spectrum. Residual atmospheric features can be more difficult to correct. One method for removing these artifacts, described by *Kelley and Gaffey* (2000), finds combinations of standard star observations taken throughout the night for which the mean, when divided into the asteroid spectrum, produces the cleanest result. Over the visible wavelength region, residual features associated with either atmospheric absorption bands or stellar lines are typically narrow, and in most cases, their presence has little impact on the interpretation of broader features contained in the asteroid spectrum. Often the points associated with these residual features can simply be omitted from the final spectrum.

Beyond the formal uncertainties that can be attached to each channel of a reduced spectrum, there is the potential for systematic offsets affecting the overall shapes of spectra, potentially impacting how these data are interpreted. The average slope of an asteroid spectrum is the characteristic that seems most sensitive to these systematic effects. While slow variations in spectral slope may be indicative of spectral heterogeneity over the surface of a rotating asteroid, sporadic fluctuations in slope are sometimes observed when a rapid sequence of spectra is taken. These fluctuations are more likely to be instrumental in nature and are most easily explained as light being preferentially lost from either the blue or red ends of the extracted spectra. Possible sources
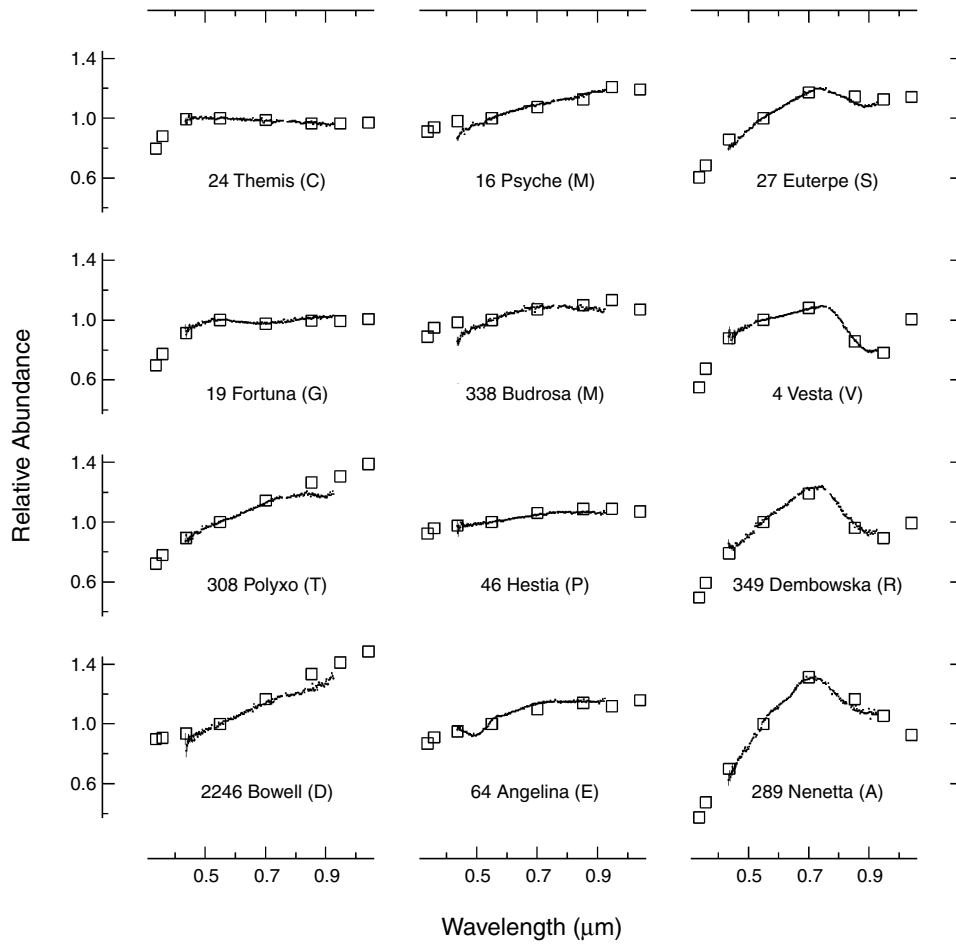
**Fig. 2.** A comparison between the Eight-Color Asteroid Survey (ECAS) colors (open squares) and SMASSII spectra (closed dots with error bars) for selected asteroids in various Tholen taxonomic classes. Those asteroids along the middle column (16 Psyche, 338 Budrosa, 46 Hestia, and 64 Angelina) show the range of spectral diversity among the Tholen X-class (E, M, and P classes, which can only be separated based on albedo) asteroids observed in the SMASSII data. Minor absorption features that are visible include the broad 0.7-μm band in the spectrum of 19 Fortuna, a 0.49-μm band in the spectrum of 64 Angelina, and a subtle 0.65-μm feature in the A-type spectrum of 289 Nenetta.

for error in the measured spectral slopes of asteroids include differential refraction (*Filippenko,* 1982) and fluctuations in seeing. Experience gained during the SMASSII survey (*Bus,* 1999) shows that while large fluctuations in spectral slope are relatively uncommon, they are more likely to be encountered under poor observing conditions that include high humidity, low-level clouds, and variable seeing.

Other likely causes for systematic offsets in asteroid spectra revolve around the methods used in correcting for atmospheric extinction, and the choice of solar analog stars. As the number of programs devoted to asteroid spectroscopy increases, the potential for systematic offsets between the various datasets is becoming more apparent. Systematic offsets in slope and in the depths and positions of bands are being routinely described when the spectra of objects observed by multiple programs are compared (*Vilas and Smith,* 1985; *Sawyer,* 1991; *Burbine,* 1999). Because of the

number of variables involved, including instrumentation, observing strategies, and reduction and calibration techniques, the source of these systematic offsets can be hard to identify. This can make the intercomparison of results obtained by different observing programs problematic, and it also underscores the significance of large-scale asteroid spectroscopy programs in which the observations and data reduction are carried out in the most internally consistent manner possible.

## 4. SPECTRAL FEATURES

The existence of absorption features in the visible-wavelength spectra of asteroids can be explained by crystal field theory and charge-transfer mechanisms (*Burns,* 1970, 1981). These absorption bands are diagnostic of particular rock-forming minerals and provide a powerful means for prob-

ing the composition of asteroid surfaces. Thorough reviews of the analyses and interpretations of asteroid spectra, based on mineralogical considerations, are presented by *Gaffey et al.* (1989, 1993a) and *Pieters and McFadden* (1994).

There are three principal features in asteroid spectra over the visible wavelengths that have remained fundamental to the description and classification of asteroids since the mid-1970s. These are (1) the presence or absence of a UV absorption feature due to strong $Fe^{2+}$ intervalence charge-transfer transitions; (2) the slope of the spectrum longward of 0.55 μm, the magnitude of which depends of the presence or absence of reddening agents such as Fe-Ni metal or organics; and (3) the presence or absence of a silicate absorption feature longward of 0.7 μm and for which the band minimum is typically centered near 1 μm. These features can be clearly seen in Fig. 2, where comparisons between ECAS colors and SMASSII spectra are plotted for asteroids belonging to various taxonomic classes as defined by *Tholen* (1984).

The increased sensitivity and spectral resolution afforded by CCD spectroscopy has also led to the identification of several weaker absorption bands in asteroid spectra. The depths of these bands range from 1% to 5% below the continuum level, and require high S/N observations for detection. Observations with somewhat higher spectral resolutions (R ~ 300–500) are often used in the study of these features to ensure the accurate calibration and removal of solar absorption lines and telluric water bands in the normalized spectra. Descriptions of the minor absorption bands recognized thus far are given below, arranged by taxonomic class:

*A-type asteroids.*   A minor absorption band, centered near 0.65 μm, is observed in the spectrum of 289 Nenetta. Laboratory spectra of olivines show the presence of this band is correlated with low forsterite:fayalite (Mg:Fe) ratios (*Sunshine et al.,* 1998).

*C-type asteroids.*   In a spectroscopic study of primitive asteroids, *Vilas and Gaffey* (1989) report the detection of a broad absorption band centered near 0.7 μm with depths of up to 5% below the continuum. This feature is attributed to the presence of phyllosilicates formed by aqueous alteration processes. The 0.7-μm feature was studied in detail by *Sawyer* (1991) and is clearly seen in the SMASSII spectrum of 19 Fortuna plotted in Fig. 2. Much weaker bands have been identified, centered at 0.43 μm (*Vilas et al.,* 1993) and at 0.60–0.65 and 0.80–0.90 μm (*Vilas et al.,* 1994), that are also associated with Fe oxide minerals produced by the aqueous alteration of anhydrous silicates.

*S-type asteroids.*   Two minor features are identified, centered near 0.60 and 0.67 μm, that are consistent with small amounts of either oxidized Fe-Ni metal or spinel-group minerals in the surface regolith (*Hiroi et al.,* 1996).

*V-type asteroids.*   A weak aborption band centered near 0.506 μm is observed in the spectrum of 4 Vesta (*Cochran and Vilas,* 1998), as illustrated in Fig. 3, and has been identified in the spectra of six other V-type asteroids belonging to the Vesta family (*Vilas et al.,* 2000). This feature is consistent with the presence of augite (a high-Ca form of pyroxene) in freshly exposed surface materials.
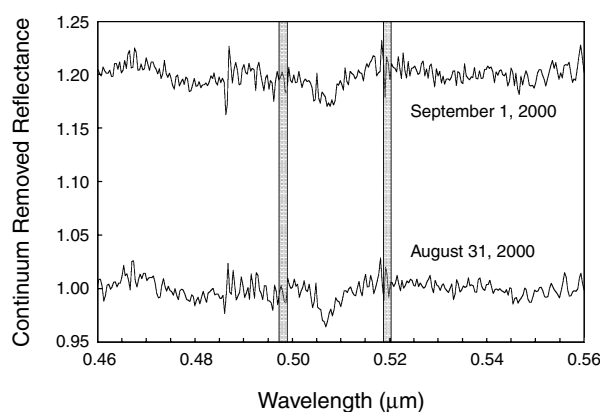


**Fig. 3.**   A magnified section of the Vesta spectrum, measured on two consecutive nights and reduced as described by *Cochran and Vilas* (1997). The spectral continuum levels have been fitted and removed, and the September 1 spectrum has been offset by 0.20 for clarity. Vertical bars show the extent of the 0.506-μm $Fe^{2+}$ pyroxene band that, because of its shape, indicates the presence of augite, a Ca-rich form of pyroxene. The strength of this feature suggests that some of the material on the surface of Vesta is relatively fresh, possibly excavated from Vesta's interior during a more recent cratering event (*Vilas et al.,* 2000).

*X-type asteroids.*   A relatively strong absorption band centered near 0.49 μm and a much weaker feature centered near 0.60 μm are observed in the spectrum of 64 Angelina, as seen in Fig. 2. More than 20 additional X-type asteroids have been identified with similar but substantially weaker features (*Bus,* 1999). *Burbine et al.* (1998) suggest that these features are consistent with the presence of the Fe sulfide mineral troilite.

## 5.   EFFECTS OF SURFACE PROPERTIES ON ASTEROID SPECTRA

Composition is the dominant factor contributing to the optical properties of an asteroid surface. However, other characteristics of the surface material can affect these optical properties and can lead to significant variations in the measured reflectance spectrum of the asteroid. Four factors are currently recognized that have the potential for altering the observed spectra:

1. *Phase reddening.*   The reddening of reflectance spectra with increased phase angle has been occasionally noted in groundbased spectrophotometric observations of asteroids (*Millis et al.,* 1976; *Bowell and Lumme,* 1979; *Murchie and Pieters,* 1996) and has been observed in laboratory measurements of meteorite and mineral powders (*Gradie et al.,* 1980; *Gradie and Veverka,* 1986). The best quantitative assessment of phase reddening on an asteroid has been made recently using results from the *NEAR Shoemaker* Near-Infrared Spectrometer observations of Eros (*Clark et al.,* 2002), which revealed a reddening of the spectral slope by 8–12% over the phase angle range of 0°–100°. To compare the colors of near-Earth asteroids with those

of asteroids near the 3:1 resonance, *Luu and Jewitt* (1990) applied nominal corrections for phase-reddening to values of the normalized reflectivity gradient (slope), S'.

2. *Space weathering.* The term "space weathering" has been used to describe the darkening and reddening of a planetary surface over time and has been applied to asteroids to help explain some of the spectral mismatches between asteroids and meteorites (e.g., *Chapman,* 1996). The processes responsible for space weathering have remained poorly defined until recently. *Moroz et al.* (1996) showed that quick melting and recrystallization of mafic materials, induced by short laser pulses, had the effect of darkening this material and increasing its spectral slope. *Yamada et al.* (1999) showed that the degree of alteration due to laser irradiation depends on mineralogy, with olivine exhibiting larger spectral variations than pyroxenes. The most recent investigations by *Pieters et al.* (2000) and *Sasaki et al.* (2001) point to the production of nanophase Fe on the surfaces of grains as the underlying cause of these alterations in spectral reflectance.

3. *Particle size.* The presence of particulate regolith on asteroid surfaces has been long known from polarimetric studies (e.g., *Dollfus et al.,* 1989) and has recently been confirmed through high-resolution spacecraft imaging of Eros (*Veverka et al.,* 2001). The size distribution of particles making up this regolith plays a significant role in the optical properties of the surface and can affect the observed spectral slope and band depths (e.g., *Johnson and Fanale,* 1973). Because of the relatively solid link between Vesta and the HED meteorites (*Binzel and Xu,* 1993), laboratory spectra of HED meteorite powders have been used to constrain the distribution of particle sizes present on the surfaces of Vesta and members of the Vesta family (*Hiroi et al.,* 1994, 1995; *Burbine et al.,* 2001).

4. *Temperature.* Depending on albedo and rotational parameters, the surface temperatures of asteroids vary from 120 K at the distance of the Jupiter Trojans to over 300 K for near-Earth asteroids (*Hinrichs et al.,* 1999). The shapes of spectral bands associated with olivines and pyroxenes are sensitive to temperature (e.g., *Roush,* 1984; *Singer and Roush,* 1985), which can affect the mineralogical interpretations of asteroid spectra (*Lucey et al.,* 1998; *Moroz et al.,* 2000).

## 6. TAXONOMY

Asteroid taxonomy has continued to evolve ever since *Chapman et al.* (1975) proposed the first classification system based on spectral reflectance properties. This evolution in taxonomy is a natural process, spurred on by the introduction of new and larger asteroid datasets and the availability of numerous classification algorithms. The history of asteroid classification has been well documented, first by *Bowell et al.* (1978) and more recently by *Tholen and Barucci* (1989), and will not be repeated here. Instead, we focus on the impact that CCD spectroscopy has had on the philosophy behind asteroid taxonomy and describe the feature-based taxonomy developed as part of the SMASSII survey (*Bus,* 1999; *Bus and Binzel,* 2002b).

Multivariate analysis techniques, such as cluster analysis, are commonly used in the derivation of taxonomic systems. For a classification to be successful, the objects being classified must cluster together in groups that are well separated in some parameter space. Based on the combined Eight-Color Asteroid Survey (ECAS) (*Zellner et al.,* 1985) and IRAS albedo (*Veeder et al.,* 1989, *Tedesco et al.*, 1992) datasets, four taxonomies have thus far been proposed: (1) the *Tholen* (1984) taxonomy, derived using a minimum spanning tree clustering algorithm; (2) the *Barucci et al.* (1987) taxonomy, derived using G-mode analysis; (3) the *Tedesco et al.* (1989) three-parameter taxonomy derived based on the visual identification of groupings in a parameter space defined by two asteroid colors and the IRAS albedos; and (4) the taxonomy of *Howell et al.* (1994) that
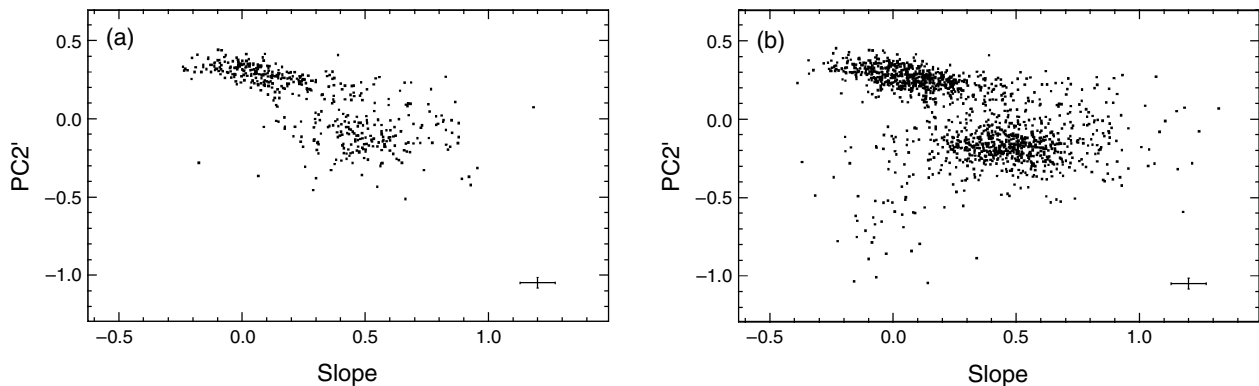


**Fig. 4.** Plots showing the distribution of the spectral components Slope and PC2' for SMASSII asteroids. The Slope parameter is defined as the average fitted slope across the entire spectrum, while PC2' is strongly correlated with the depth of the 1-μm band, with lower values of PC2' corresponding to increased band depth. Error bars shown in the lower right corner of each plot represent the $1\sigma$ uncertainty in the component score for an object observed only once. **(a)** Plot of only the brighter SMASSII asteroids also observed during ECAS. **(b)** Plot of all SMASSII asteroids. The increased dispersion of points plotted is indicative of the greater diversity in spectral properties observed as smaller asteroids are measured.

TABLE 1.   Summary of taxonomic classes.

| Tholen Class | Barucci Class | Howell Class | SMASSII Class | Description |
|---|---|---|---|---|
| B, F | B0–B3 | B + F | B | Linear, featureless spectrum with bluish to neutral slope |
| | | | Cb | Similar to B spectrum with neutral to slight reddish slope |
| G | G0 | Cv, Cx | Cg | Strong absorption ($\lambda < 0.55$ μm), and featureless with neutral to reddish slope ($\lambda > 0.55$ μm) |
| | | | Cgh | Similar to Cg spectrum, with shallow absorption centered near 0.7 μm |
| C | | | C | Weak to medium absorption ($\lambda < 0.55$ μm), neutral to slightly reddish and featureless ($\lambda > 0.55$ μm) |
| | C0 | | Ch | Similar to C spectrum, with shallow absorption centered near 0.7 μm |
| E, M, P | E0, M0 | E. M, P | Xc | Slightly reddish spectrum, featureless except for broad convex curvature centered near 0.7 μm |
| | | | Xk | Similar to Xc spectrum, but redder slope ($\lambda < 0.7$ μm), and generally flat ($\lambda > 0.7$ μm) |
| | | | X | Generally featureless, linear spectrum with slight to moderate reddish slope |
| | | | Xe | Overall slope slight to moderately red, concave absorption feature centered near 0.5 μm, with occasional secondary absorption centered near 0.6 μm |
| T | D0–D3 | T | T | Moderately reddish slope ($\lambda < 0.75$ μm), and generally flat ($\lambda > 0.85$ μm) |
| D | | D | D | Relatively featureless spectrum with very steep red slope |
| S | S0–S3 | K | K | Moderately steep red slope ($\lambda < 0.75$ μm) and flat to slightly bluish ($\lambda > 0.75$ μm) |
| | | So | L | Very steep red slope ($\lambda < 0.75$ μm) and flat to slightly bluish ($\lambda > 0.75$ μm) |
| | | | Ld | Similar to L spectrum, but steeper red slope ($\lambda < 0.75$ μm) |
| | | | Sa | Similar to S spectrum, but with steeper slope ($\lambda < 0.7$ μm) |
| | | | Sl | Similar to S spectrum, but with steeper slope ($\lambda < 0.7$ μm) and a shallower absorption ($\lambda > 0.75$ μm) |
| | | S | S | Moderately steep, reddish slope ($\lambda < 0.7$ μm), and a moderate to deep absorption band ($\lambda > 0.75$ μm) |
| | | | Sr | Similar to S spectrum, but with very steep red slope ($\lambda < 0.7$ μm) and a deeper absorption ($\lambda > 0.75$ μm) |
| | | Sp | Sk | Similar to S spectrum, but with shallower reddish slope ($\lambda < 0.7$ μm) and a shallower absorption ($\lambda > 0.75$ μm) |
| | | | Sq | Similar to S spectrum, but with shallower reddish slope ($\lambda < 0.7$ μm) |
| Q | — | — | Q | Moderately steep red slope ($\lambda < 0.7$ μm) and a deep, very rounded absorption feature ($\lambda > 0.75$ μm) |

TABLE 1.   (continued).

| Tholen Class | Barucci Class | Howell Class | SMASSII Class | Description |
|---|---|---|---|---|
| A | A0 | A | A | Very steep to extremely steep red slope ($\lambda < 0.75$ μm) and a moderately deep absorption ($\lambda > 0.75$ μm). Reflectance maximum or 1 μm feature usually more rounded than in S-type spectrum |
| R | V0 | R | R | Very steep red slope ($\lambda < 0.7$ μm) and a deep absorption feature ($\lambda > 0.75$ μm). Reflectance maximum more sharply peaked than in S-type spectra |
| V | V0 | V | V | Moderate to very steep red slope ($\lambda < 0.7$ μm) with an extremely deep absorption band ($\lambda > 0.75$ μm) |
| — | — | — | O | Moderately red slope ($\lambda < 0.55$ μm), then less steep ($0.55 < \lambda < 0.7$ μm). Deep absorption ($\lambda > 0.75$ μm) |

implemented artificial neural networks to separately analyze the ECAS data and the combined data from ECAS and the 52-color asteroid survey (*Bell et al.,* 1988). The taxonomies resulting from these four studies are fundamentally similar, suggesting that statistically significant boundaries exist between clusters of objects in the combined ECAS/IRAS dataset and that the classification results are relatively insensitive to the choice of clustering methods used.

Initial analysis of the SMASSII spectra (*Bus,* 1999) revealed a conspicuous absence of gaps separating spectral types, with the only significant void being that separating the asteroids whose spectra contain a 1-μm silicate band from those that do not. The spectral component plots shown in Fig. 4 indicate an overall increase in spectral diversity, as smaller asteroids are included. The apparent continuum of objects in spectral component space depicted in Fig. 4b is verified by the continua in spectral features observed in asteroid families (e.g., *Doressoundiram et al.,* 1998; *Lazzaro et al.,* 1999) and between previously defined taxonomic classes (*Binzel et al.,* 1996). Various attempts to classify the SMASSII spectra using clustering techniques were unsuccessful, usually resulting in the identification of two very large classes, and a number of small groupings consisting of outlying objects. These initial results prompted a reassessment of the goals of asteroid classification and ultimately led to the development of a new feature-based taxonomy.

Development of the SMASSII taxonomy was based on five principles: (1) The established framework provided by the Tholen taxonomy was utilized in an attempt to preserve the historic structure and spirit of past asteroid taxonomies. (2) The SMASSII classes were defined solely on the presence (or absence) of absorption features contained in the visible-wavelength spectra. (3) The classes were arranged in a way that reflects the spectral continuum revealed by the SMASSII data. (4) To properly parameterize the various spectral features, different analytical and multivariate analysis techniques were used in the classification of the SMASSII asteroids. Because some spectral features are very subtle and not easily parameterized, the classification procedures allowed for visual inspection of the data and for some class labels to be assigned based on human judgment. (5) When possible, the sizes (scale-lengths) and boundaries of the taxonomic classes were defined based on the spectral variance observed in natural groupings among the asteroids, such as dynamical families.

The SMASSII taxonomy consists of 26 classes. Several of the smaller classes defined by Tholen, such as the A, Q, R, V, D, and T classes remain unchanged in the SMASSII system. Larger associations such as the S and C "complexes" have been subdivided. The X-type asteroids were described by Tholen as being spectrally degenerate, and could only be subdivided into the E, M, and P classes based on albedo. However, the SMASSII spectra reveal subtle variations among the members of the X complex, allowing these objects to be divided into four classes based solely on spectral features. Descriptions of the SMASSII classes are given in Table 1, along with comparisons to previous (*Tholen,* 1984; *Barucci et al.,* 1987; *Howell et al.,* 1994) taxonomies. The continuum in spectral properties represented by the SMASSII taxonomy is depicted in Fig. 5.

One drawback of the SMASSII taxonomy is that applying this system to newly observed asteroids can be cumbersome. Various descriptions of the SMASSII spectral classes such as those provided in Table 1 and elsewhere (*Bus,* 1999; *Bus and Binzel* 2002b) allow for the classification of individual objects. However, a more automated approach, such as that provided by a neural network (*Bus and Binzel,* 2000) is required if this taxonomy is to be readily applied to large datasets. An important factor to consider is the uncertainty associated with taxonomic labels. The classification assigned to an asteroid is only as good as the observational data. If subsequent observations of an asteroid reveal variations in its spectrum, whether due to compositional heterogeneity over the surface of the asteroid, variations in viewing geometry, or systematic offsets in the observations themselves, the taxonomic label may change.
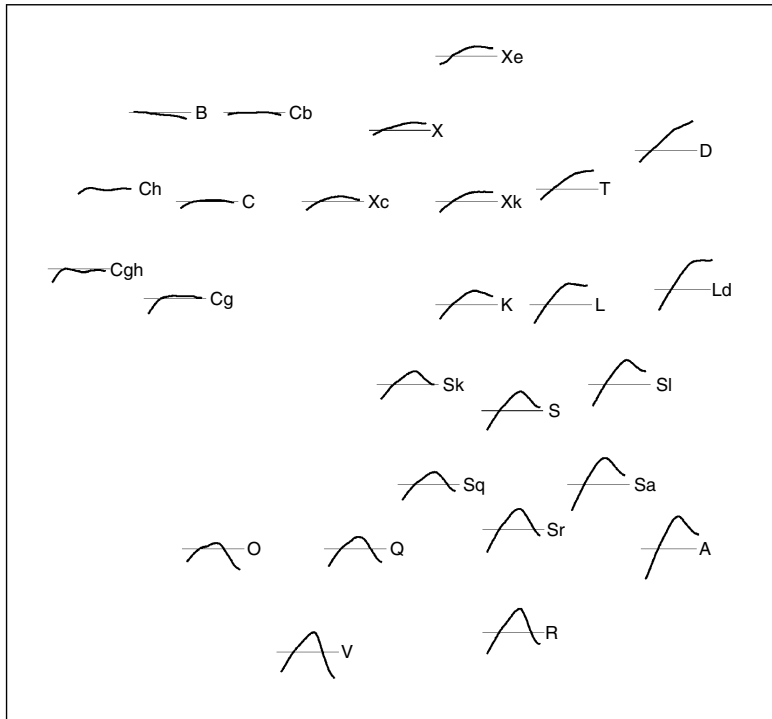
**Fig. 5.** Diagram showing all 26 SMASSII taxonomic classes, from *Bus and Binzel* (2002b). The spectra are arranged in a pattern that approximates the location of each class in spectral component space. The average spectral slope increases from left to right, and the depth of the 1-μm silicate absorption band generally increases from top to bottom.

When this occurs, we should not feel compelled to decide which label is "correct," but should rather accept these distinct labels as a consequence of our growing knowledge about that object.

## 7.  NEAR-INFRARED SPECTROSCOPY

Just as CCDs have revolutionized visible-wavelength spectroscopy, the introduction of new generation near-infrared array detectors (*Hodapp,* 2000) is providing the capability of obtaining high-quality spectra of asteroids out to 2.5 μm and beyond. A new low- to medium-resolution NIR spectrograph and imager, called SpeX, is now in use at the NASA Infrared Telescope Facility (IRTF) on Mauna Kea (*Rayner et al.,* 1998). SpeX is capable of low-resolution spectroscopy (R ~ 50–250) over the wavelength range of 0.8–2.5 μm, while in a higher-resolution (R ≤ 2500) cross-dispersed mode, the spectral coverage is extended to 5.5 μm. SpeX is just one of a number of NIR spectrographs being designed and built at observatories around the world. Because the NIR region (~1–4 μm) contains absorption bands that are fundamental to studies of mineralogy (*Gaffey et al.,* 1989), these instruments could have an even greater impact on asteroid studies than CCD spectrographs.

The observing strategies and data-reduction techniques used in measuring the NIR spectra of asteroids are similar to those described earlier for CCD spectroscopy. The calibration of these data is complicated, however, by an increase in the number and relative strengths of night-sky emission lines and by the presence of strong telluric absorption bands due to atmospheric $H_2O$ and $CO_2$. The depths of these absorption bands are sensitive to the amount of pre-

cipitable water in the atmosphere above the observer and can vary rapidly as sky conditions change. As discussed earlier, one method for minimizing the effects of telluric absorption bands is based on combining numerous solar-like star spectra and finding an average in which the absorption band depths most closely match those in the asteroid spectrum (*Kelley and Gaffey,* 2000). Another approach is based on nightly observations of stars belonging to the spectral class A0. The spectra of these stars are nearly featureless and can therefore be used to determine the profiles and relative strengths of absorption bands caused by Earth's atmosphere. By scaling these telluric features to match the band depths in each asteroid and solar-star spectrum, the presence of residual atmospheric features in a normalized asteroid spectrum can be minimized. A similar method uses a model of atmospheric transmission like that produced by the ATRAN software package (*Lord,* 1992). Using this algorithm, the amount of precipitable water can be varied, allowing the structure of atmospheric absorption features to be fitted and removed from each observation prior to dividing the asteroid spectrum by that of the solar-like star.

Due to the strengths and complex structure of the major telluric bands, proper wavelength calibration of both the asteroid and standard star spectra is crucial. Minor offsets in wavelength between the spectra can result in significant residuals in the normalized asteroid spectrum. These wavelength offsets are usually measured in small fractions of a pixel and are commonly associated with instrument flexure. These offsets can be corrected by shifting one of the spectra with respect to the other, where the magnitude and direction of the shift is usually determined by cross-correlating the absorption features contained in the spectra.

# 8.  DISCUSSION

The widespread availability of CCD spectrographs has resulted in a wealth of spectroscopic data on asteroids. Long-term observing programs, in which the same instrumentation, observing strategies, and reduction techniques are used, are particularly valuable, as these are capable of producing large, internally consistent sets of asteroid spectra. The largest spectroscopic surveys to date include (1) a survey of low-albedo asteroids by *Sawyer* (1991), which contains observations of 115 asteroids; (2) the first phase of the Small Main-belt Asteroid Spectroscopic Survey (SMASSI) with 316 asteroids observed (*Xu et al.,* 1995); (3) SMASSII, with 1447 objects observed (*Bus and Binzel,* 2002a); and (4) the Small Solar System Objects Spectroscopic Survey (S³OS²) by *Lazzaro et al.* (2001), an ongoing survey that has already produced measurements for 800 asteroids. The combined efforts of these surveys along with several smaller studies have produced spectral measurements for an estimated 3000 individual asteroids. Even so, there are tens of thousands of additional main-belt asteroids that could become bright enough to be within reach of a 4-m class telescope, but which currently lack any spectroscopic measurements.

The applications of spectroscopy to studies of the origin and evolution of the asteroids are numerous. As the number of asteroids with measured spectra increases, bias-corrected models of the compositional structure of the asteroid belt can be refined (*Gradie et al.,* 1989; *Bus,* 1999), and unusual occurrences of objects can be identified. One such example is the V-type asteroid 1459 Magnya, an outer main-belt object (at 3.15 AU) whose basaltic nature was recently identified from spectral observations (*Lazzaro et al.,* 2000). All other known V-class asteroids are associated with the Vesta family (*Binzel and Xu,* 1993) and are confined to the inner main belt between 2.2 and 2.5 AU. Anomalous spectral types are also bound to be discovered, like that measured for asteroid 3628 Boznemcova (*Binzel et al.,* 1993), which led to the creation of a new taxonomic O class.

Recent spectroscopic studies of dynamical asteroid families have revealed strong similarities between the members of each family (e.g., *Doressoundiram et al.,* 1998; *Lazzaro et al.,* 1999; *Bus,* 1999). These findings have helped confirm the genetic reality of asteroid families and can be used to place constraints on collisional and dynamical models of family formation, as discussed by *Cellino et al.* (2002). Asteroid families provide unique opportunities to peer into the interiors of once-larger parent bodies and to search for spectral (compositional) heterogeneity among the members. Rotationally resolved spectra of individual asteroids can also be searched for evidence of spectral variation over their surfaces (*Murchie and Pieters,* 1996; *Cochran and Vilas,* 1998; *Mothé-Diniz et al.,* 2000; *Howell et al.,* 2001).

Close approaches by near-Earth objects (NEOs) provide opportunities to measure the spectral properties of very small bodies, many with diameters much smaller than 1 km. Spectral studies of NEOs are crucial for understanding their compositional distributions and for tracing origins of these objects to source regions in the main belt (*Binzel et al.,* 1996; *Hammergren,* 1998; *Hicks et al.,* 1998) and within the comet population (e.g., *Chamberlin et al.,* 1996). A fundamental goal of asteroid spectroscopy is to establish links between meteorites and the asteroids (or asteroid classes) from which they were derived. These identifications allow meteorites to be placed into a geologic context while constraining the composition and thermal histories of the asteroidal parent bodies (*Lipschutz et al.,* 1989; *Pieters and McFadden,* 1994). While some credible links have been identified between specific meteorite and asteroid classes (see *Burbine et al.,* 2002), much work remains before a consistent picture of the asteroid belt emerges that is based on both asteroid and meteorite evidence (*Bell et al.,* 1989; *Cellino,* 2000).

By combining results from visible and NIR spectroscopy, questions regarding mineralogy can be more fully addressed. The spectral interval between 0.7 and 2.5 μm is particularly important to studies of silicate minerals, such as pyroxenes, olivines and plagioclase, due to fundamental absorption bands centered near 1 and 2 μm (e.g., *Burns,* 1970; *Adams,* 1974, 1975; *Cloutis et al.,* 1986). The ability to obtain high-quality spectra over this interval is prompting the use of more advanced spectral analysis techniques, like the Modified Gaussian Model (MGM) (*Sunshine et al.,* 1990), to deconvolve individual absorption bands associated with the different silicate mineral phases. Reliable estimates of silicate mineralogy are key to constraining the thermal histories of silicate-rich asteroids and are helping to clarify the petrologic nature of the S-type asteroids (*Gaffey et al.,* 1993b; *Sunshine et al.,* 2002). The spectral window between 2.5 and 3.5 μm is significant to studies of hydrated minerals on asteroids, due to absorption bands centered near 3 μm that are associated with bound water and structural OH found in hydrated silicates (e.g., *Lebofsky et al.,* 1981; *Jones et al.,* 1990; *King et al.,* 1992). Together with visible-wavelength observations of the 0.7-μm phyllosilicate feature (*Vilas and Gaffey,* 1989; *Vilas and Sykes,* 1996; *Barucci et al.,* 1998), measurements of the 3-μm absorption band can be used to map the spatial extent of aqueous alteration on surfaces of asteroids and to constrain the heating mechanisms that led to this alteration, as discussed in *Rivkin et al.* (2002). With the addition of NIR spectra, asteroid taxonomy will also likely benefit as new classification schemes will ultimately be developed that are more representative of mineralogy.

## REFERENCES

Adams J. B. (1974) Visible and near-infrared diffuse reflectance spectra of pyroxenes as applied to remote sensing of solid objects in the solar system. *J. Geophys. Res., 79,* 4829–4836.

Adams J. B. (1975) Interpretation of visible and near-infrared diffuse reflectance spectra of pyroxenes and other rock-forming minerals. In *Infrared and Raman Spectroscopy of Lunar and Terrestrial Minerals* (C. Karr, ed.), pp. 91–116. Academic, New York.

Barucci M. A., Capria M. T., Coradini A., and Fulchignoni M. (1987) Classification of asteroids using G-mode analysis.

*Icarus, 72,* 304–324.

Barucci M. A., Doressoundiram A., Fulchignoni M., Florczak M., Lazzarin M., Angeli C., and Lazzaro D. (1998) Search for aqueously altered materials on asteroids. *Icarus, 132,* 388–396.

Bell J. F., Owensby P. D., Hawke B. R., and Gaffey M. J. (1988) The 52-color asteroid survey: Final results and interpretation (abstract). In *Lunar and Planetary Science XIX,* pp. 57–58. Lunar and Planetary Institute, Houston.

Bell J. F., Davis D. R, Hartmann W. K., and Gaffey M. J. (1989) Asteroids: The big picture. In *Asteroids II* (R. P. Binzel et al., eds.), pp. 921–945. Univ. of Arizona, Tucson.

Binzel R. P. and Xu S. (1993) Chips off of asteroid 4 Vesta: Evidence for the parent body of basaltic achondrite meteorites. *Science, 260,* 186–191.

Binzel R. P., Xu S., Bus S. J., Skrutskie M. F., Meyer M. R., Knezek P., and Barker E. S. (1993) Discovery of a main-belt asteroid resembling ordinary chondrite meteorites. *Science, 262,* 1541–1543.

Binzel R. P., Bus S. J., Burbine T. H., and Sunshine J. M. (1996) Spectral properties of near-Earth asteroids: Evidence for sources of ordinary chondrite meteorites. *Science, 273,* 946–948.

Bobrovnikoff N. T. (1929) The spectra of minor planets. *Lick Obs. Bull., 14,* 18–27.

Bowell E. and Lumme K. (1979) Colorimetry and magnitudes of asteroids. In *Asteroids* (T. Gehrels, ed.), pp. 132–169. Univ. of Arizona, Tucson.

Bowell E., Chapman C. R., Gradie J. C., Morrison D., and Zellner B. (1978) Taxonomy of asteroids. *Icarus, 35,* 313–335.

Burbine T. H. (1999) Forging asteroid-meteorite relationships through reflectance spectroscopy. Ph.D. thesis, Massachusetts Institute of Technology, Cambridge.

Burbine T. H., Cloutis E. A., Bus S. J., Meibom A., and Binzel R. P. (1998) The detection of troilite (FeS) on the surfaces of E-class asteroids (abstract). *Bull. Am. Astron. Soc., 30,* 1025–1026.

Burbine T. H., Buchanan P. C., Binzel R. P., Bus S. J., Hiroi T., Hinrichs J. L., Meibom A., and McCoy T. J. (2001) Vesta, Vestoids, and the howardite, eucrite, diogenite group: Relationships and the origin of spectral features. *Meteoritics & Planet. Sci., 36,* 761–781.

Burbine T. H., McCoy T. J., Meibom A., Gladman B., and Keil K. (2002) Meteoritic parent bodies: Their number and identification. In *Asteroids III* (W. F. Bottke Jr. et al., eds.), this volume. Univ. of Arizona, Tucson.

Burns R. G. (1970) *Mineralogical Applications of Crystal Field Theory.* Cambridge Univ., New York. 224 pp.

Burns R. G. (1981) Intervalence transitions in mixed-valence mainerals of iron and titanium. *Annu. Rev. Earth Planet. Sci., 9,* 345–383.

Bus S. J. (1999) Compositional structure in the asteroid belt: Results of a spectroscopic survey. Ph.D. thesis, Massachusetts Institute of Technology, Cambridge.

Bus S. J. and Binzel R. P. (2000) A neural network simulation of the SMASSII asteroid taxonomy (abstract). *Bull. Am. Astron. Soc., 32,* 1004.

Bus S. J. and Binzel R. P. (2002a) Phase II of the Small Main-Belt Asteroid Spectroscopic Survey: The observations. *Icarus, 158,* 106–145.

Bus S. J. and Binzel R. P. (2002b) Phase II of the Small Main-Belt Asteroid Spectroscopic Survey: A feature-based taxonomy. *Icarus, 158,* 146–177.

Cellino A. (2000) Minor bodies: Spectral gradients and relation-ships with meteorites. *Space Sci. Rev., 92,* 397–412.

Cellino A., Bus S. J., Doressoundiram A., and Lazzaro D. (2002) Spectroscopic properties of asteroid families. In *Asteroids III* (W. F. Bottke Jr. et al., eds.), this volume. Univ. of Arizona, Tucson.

Chamberlin A. B., McFadden L. A., Schulz R., Schleicher D. G., and Bus S. J. (1996) 4015 Wilson-Harrington, 2201 Oljato, and 3200 Phaethon: Search for CN emission. *Icarus, 119,* 173–181.

Chapman C. R. (1996) S-type asteroids, ordinary chondrites, and space weathering: The evidence from Galileo's fly-bys of Gaspra and Ida. *Meteoritics, 31,* 699–725.

Chapman C. R. and Gaffey M. J. (1979) Reflectance spectra for 277 asteroids. In *Asteroids* (T. Gehrels, ed.), pp. 655–687. Univ. of Arizona, Tucson.

Chapman C. R., Johnson T. V., and McCord T. B. (1971) A review of spectrophotometric studies of asteroids. In *Physical Studies of Minor Planets* (T. Gehrels, ed.), pp. 51–65. NASA SP-267, Washington, DC.

Chapman C. R., Morrison D., and Zellner B. (1975) Surface properties of asteroids: A synthesis of polarimetry, radiometry, and spectrophotometry. *Icarus, 25,* 104–130.

Clark B. E., Helfenstein P., Bell J. F. III, Peterson C., Veverka J., Izenberg N. I., Domingue D., Wellnitz D., and McFadden L. (2002) NEAR Infrared Spectrometer photometry of asteroid 433 Eros. *Icarus, 155,* 189–204.

Cloutis E. A., Gaffey M. J., Jackowski T. L., and Reed K. L. (1986) Calibrations of phase abundance, composition, and particle size distribution for olivine-orthopyroxene mixtures from reflectance spectra. *J. Geophys. Res., 91,* 11641–11653.

Cochran A. L. and Vilas F. (1997) The McDonald Observatory serendipitous UV/blue spectral survey of asteroids. *Icarus, 127,* 121–129.

Cochran A. L. and Vilas F. (1998) The changing spectrum of Vesta: Rotationally resolved spectroscopy of pyroxene on the surface. *Icarus, 134,* 207–212.

Dollfus A., Wolff M., Geake J. E., Lupishko D. F., and Dougherty L. M. (1989) Photopolarimetry of asteroids. In *Asteroids II* (R. P. Binzel et al., eds.), pp. 594–616. Univ. of Arizona, Tucson.

Doressoundiram A., Barucci M. A., Fulchignoni M., and Florczak M. (1998) Eos family: A spectroscopic study. *Icarus, 131,* 15–31.

Filippenko A. V. (1982) The importance of atmospheric differential refraction in spectroscopy. *Publ. Astron. Soc. Pac., 94,* 715–721.

Gaffey M. J. and McCord T. B. (1979) Mineralogical and petrological characterization of asteroid surface materials. In *Asteroids* (T. Gehrels, ed.), pp. 688–723. Univ. of Arizona, Tucson.

Gaffey M. J., Bell J. F., and Cruikshank D. P. (1989) Reflectance spectroscopy and asteroid surface mineralogy. In *Asteroids II* (R. P. Binzel et al., eds.), pp. 98–127. Univ. of Arizona, Tucson.

Gaffey M. J., Burbine T. H., and Binzel R. P. (1993a) Asteroid spectroscopy: Progress and perspectives. *Meteoritics, 28,* 161–187.

Gaffey M. J., Bell J. F., Brown R. H., Burbine T. H., Piatek J. L., Reed K. L., and Chaky D. A. (1993b) Mineralogical variations within the S-type asteroid class. *Icarus, 106,* 573–602.

Gradie J. and Veverka J. (1986) The wavelength dependence of phase coefficients. *Icarus, 66,* 455–467.

Gradie J., Veverka J., and Buratti B. (1980) The effects of scattering geometry on the spectrophotometric properties of powdered material. *Proc. Lunar Planet. Sci. Conf. 11th,* pp. 799–815.

Gradie J. C., Chapman C. R., and Tedesco E. F. (1989) Distribution of taxonomic classes and the compositional structure of

the asteroid belt. In *Asteroids II* (R. P. Binzel et al., eds.), pp. 316–335. Univ. of Arizona, Tucson.

Hammergren M. (1998) The composition of near-Earth objects. Ph.D. thesis, University of Washington, Seattle.

Hardorp J. (1978) The sun among the stars. I–A search for solar spectral analogs. *Astron. Astrophys., 63,* 383–390.

Hayes D. S. and Latham D. W. (1975) A rediscussion of the atmospheric extinction and the absolute spectral-energy distribution of Vega. *Astrophys. J., 197,* 593–601.

Hicks M. D., Fink U., and Grundy W. M. (1998) The unusual spectra of 15 near-Earth asteroids and extinct comet candidates. *Icarus, 133,* 69–78.

Hinrichs J. L., Lucey P. G., Robinson M. S., Meibom A., and Krot A. N. (1999) Implications of temperature-dependent near-IR spectral properties of common minerals and meteorites for remote sensing of asteroids. *Geophys. Res. Lett., 26,* 1661–1664.

Hiroi T., Pieters C. M., and Takeda H. (1994) Grain size of the surface regolith of asteroid 4 Vesta estimated from its reflectance spectrum in comparison with HED meteorites. *Meteoritics, 29,* 394–396.

Hiroi T., Binzel R. P., Sunshine J. M., Pieters C. M., and Takeda H. (1995) Grain sizes and mineral compositions of surface regoliths of Vesta-like asteroids. *Icarus, 115,* 374–386.

Hiroi T., Vilas F., and Sunshine J. M. (1996) Discovery and analysis of minor absorption bands in S-asteroid visible reflectance spectra. *Icarus, 119,* 202–208.

Hodapp K. W. (2000) Near-infrared detector arrays:  Current state of the art. *Proc. SPIE, 4008,* 1228–1239.

Howell E. S., Merényi E., and Lebofsky L. A. (1994) Classification of asteroid spectra using a neural network. *J. Geophys. Res., 99,* 10847–10865.

Howell E. S., Rivkin A. S., Vilas F., and Soderberg A. M. (2001) Aqueous alteration in low albedo asteroids (abstract). In *Lunar and Planetary Science XXXII,* Abstract #2058. Lunar and Planetary Institute, Houston (CD-ROM).

Janesick J. and Elliott T. (1992) History and advancements of large area array scientific CCD imagers. In *Astronomical CCD Observing and Reduction Techniques* (S. B. Howell, ed.), pp. 1–67. ASP Conference Series 23.

Johnson T. V. and Fanale F. P. (1973) Optical properties of carbonaceous chondrites and their relationship to asteroids. *J. Geophys. Res., 78,* 8507–8518.

Jones T. D., Lebofsky L. A., Lewis J. S., and Marley M. S. (1990) The composition and origin of the C, P, and D asteroids:  Water as a tracer of thermal evolution in the outer belt. *Icarus, 88,* 172–192.

Kelley M. S. and Gaffey M. J. (2000) 9 Metis and 113 Amalthea:  A genetic asteroid pair. *Icarus, 144,* 27–38.

King T. V. V., Clark R. N., Calvin W. M., Sherman D. M., and Brown R. H. (1992) Evidence for ammonium-bearing minerals on Ceres. *Science, 255,* 1551–1553.

Lazzaro D., Mothé-Diniz T., Carvano J. M., Angeli C. A., Betzler A. S., Florczak M., Cellino A., Di Martino M., Doressoundiram A., Barucci M. A., Dotto E., and Bendjoya P. (1999) The Eunomia family:  A visible spectroscopic survey. *Icarus, 142,* 445–453.

Lazzaro D., Michtchenko T., Carvano J. M., Binzel R. P., Bus S. J., Burbine T. H., Mothé-Diniz T., Florczak M., Angeli C. A., and Harris A. W. (2000) Discovery of a basaltic asteroid in the outer main belt. *Science, 288,* 2033–2035.

Lazzaro D., Carvano J. M., Mothé-Diniz T., Angeli C., and Florczak M. (2001) S3OS2:  A visible spectroscopic survey of around 800 asteroids (abstract). In *Asteroids 2001:  From Piazzi to the 3rd Millennium,* p. 174. Osservatorio di Palermo, Sicily.

Lebofsky L. A., Feierberg M. A., Tokunaga A. T., Larson H. P., and Johnson J. R. (1981) The 1.7- to 4.2-μm spectrum of asteroid 1 Ceres:  Evidence for structural water in clay minerals. *Icarus, 48,* 453–459.

Lipschutz M. E., Gaffey M. J., and Pellas P. (1989) Meteoritic parent bodies:  Nature, number, size and relation to present-day asteroids. In *Asteroids II* (R. P. Binzel et al., eds.), pp. 740–777. Univ. of Arizona, Tucson.

Lord S. D. (1992) *A New Software Tool for Computing Earth's Atmospheric Transmission of Near- and Far-Infrared Radiation.* NASA TM-103957. NASA Ames Research Center, Moffett Field, California.

Lucey P. G., Keil K., and Whitely R. (1998) The influence of temperature on the spectra of the A-asteroids and implications for their silicate chemistry. *J. Geophys. Res., 103,* 5865–5871.

Luu J. X. and Jewitt D. C. (1990) Charge-coupled device spectra of asteroids. I. Near-Earth and 3:1 resonance asteroids. *Astron. J., 99,* 1985–2011.

McCord T. B., Adams J. B., and Johnson T. V. (1970) Asteroid Vesta:  Spectral reflectivity and compositional implications. *Science, 168,* 1445–1447.

Millis R. L., Bowell E., and Thompson D. T. (1976) UBV photometry of asteroid 433 Eros. *Icarus, 28,* 53–67.

Moroz L. V., Fisenko A. V., Semjonova L. F., Pieters C. M., and Korotaeva N. N. (1996) Optical effects of regolith processes on S-asteroids as simulated by laser shots on ordinary chondrite and other mafic materials. *Icarus, 122,* 366–382.

Moroz L., Schade U., and Wasch R. (2000) Reflectance spectra of olivine-orthopyroxene-bearing assemblages at decreased temperatures:  Implications for remote sensing of asteroids. *Icarus, 147,* 79–93.

Mothé-Diniz T., Lazzaro D., Carvano J. M., and Florczak M. (2000) Rotationally resolved spectra of some S-type asteroids. *Icarus, 148,* 494–507.

Murchie S. L. and Pieters C. M. (1996) Spectral properties and rotational spectral heterogeneity of 433 Eros. *J. Geophys. Res., 101,* 2201–2214.

Pieters C. M. and McFadden L. A. (1994) Meteorite and asteroid reflectance spectroscopy:  Clues to early solar system processes. *Annu. Rev. Earth Planet. Sci., 22,* 457–497.

Pieters C. M., Taylor L. A., Noble S. K., Keller L. P., Hapke B., Morris R. V., Allen C. C., McKay D. S., and Wentworth S. (2000) Space weathering on airless bodies:  Resolving a mystery with lunar samples. *Meteoritcs & Planet. Sci., 35,* 1101–1107.

Rayner J. T., Toomey D. W., Onaka P. M., Denault A. J., Stahlberger W. E., Watanabe D. Y., and Wang S.-I. (1998) SpeX:  A medium-resolution IR spectrograph for IRTF. *Proc. SPIE, 3354,* 468–479.

Rivkin A. S., Howell E. S., Vilas F., and Lebofsky L. A. (2002) Hydrated minerals on asteroids:  The astronomical record. In *Asteroids III* (W. F. Bottke Jr. et al., eds.), this volume. Univ. of Arizona, Tucson.

Roush T. L. (1984) Effects of temperature on remotely sensed mafic mineral absorption features. M.S. thesis, University of Hawai'i, Honolulu.

Sasaki S., Nakamura K., Hamabe Y., Kurahashi E., and Hiroi T. (2001) Production of iron nanoparticles by laser irradiation in a simulation of lunar-like space weathering. *Nature, 410,* 555–557.

Sawyer S. R. (1991) A high resolution CCD spectroscopic survey

of low albedo main belt asteroids. Ph.D. thesis, University of Texas, Austin.

Singer R. B. and Roush T. L. (1985) Effects of temperature on remotely sensed mineral absorption features. *J. Geophys. Res., 90,* 12434–12444.

Sunshine J. M., Pieters C. M., and Pratt S. F. (1990) Deconvolution of mineral absorption bands: An improved approach. *J. Geophys. Res., 95,* 6955–6966.

Sunshine J. M., Binzel R. P., Burbine T. H., and Bus S. J. (1998) Is asteroid 289 Nenetta compositionally analogous to the Brachinite meteorites? (abstract). In *Lunar and Planetary Science XXIX,* Abstract #1430. Lunar and Planetary Institute, Houston (CD-ROM).

Sunshine J. M, Bus S. J., Burbine T. H., McCoy T. J., and Binzel R. P. (2002) Unambiguous spectral evidence for high- (and low-) calcium pyroxene in asteroids and meteorites (abstract). In *Lunar and Planetary Science XXXIII,* Abstract #1356. Lunar and Planetary Institute, Houston (CD-ROM).

Tedesco E. F., Williams J. G., Matson D. L., Veeder G. J., Gradie J. C., and Lebofsky L. A. (1989) A three-parameter asteroid taxonomy. *Astron. J., 97,* 580–606.

Tedesco E., Veeder G., Fowler J., and Chillemi J. (1992) *The IRAS Minor Planet Survey.* Phillips Lab PL-TR-92-2049, Hanscom Air Force Base, Massachusetts.

Tholen D. J. (1984) Asteroid taxonomy from cluster analysis of photometry. Ph.D. thesis, University of Arizona, Tucson.

Tholen D. J. and Barucci M. A. (1989) Asteroid taxonomy. In *Asteroids II* (R. P. Binzel et al., eds.), pp. 298–315. Univ. of Arizona, Tucson.

Veeder G. J., Tedesco E. F. and Matson D. L. (1989) Asteroid results from the IRAS survey. In *Asteroids II* (R. P. Binzel et al., eds.), pp. 282–289. Univ. of Arizona, Tucson.

Veverka J., Thomas P. C., Robinson M., Murchie S., Chapman C., Bell M., Harch A., Merline W. J., Bell J. F., Bussey B., Carcich B., Cheng A., Clark B., Domingue D., Dunham D., Farquhar R., Gaffey M. J., Hawkins E., Izenberg N., Joseph J., Kirk R., Li H., Lucey P., Malin M., McFadden L., Miller J. K., Owen W. M., Peterson C., Prockter L., Warren J., Wellnitz D., Williams B. G., and Yeomans D. K. (2001) Imaging of small-scale features on 433 Eros from NEAR: Evidence for a complex regolith. *Science, 292,* 484–488.

Vilas F. and Gaffey M. J. (1989) Phyllosilicate absorption features in main-belt and outer-belt asteroid reflectance spectra. *Science, 246,* 790–792.

Vilas F. and Smith B. A. (1985) Reflectance spectrophotometry (~0.5–1.0 μm) of outer-belt asteroids: Implications for primitive, organic solar system material. *Icarus, 64,* 503–516.

Vilas F. and Sykes M. V. (1996) Are low-albedo asteroids thermally metamorphosed? *Icarus, 124,* 483–489.

Vilas F., Larson S. M., Hatch E. C., and Jarvis K. S. (1993) CCD reflectance spectra of selected asteroids. II. Low-albedo asteroid spectra and data extraction techniques. *Icarus, 105,* 67–78.

Vilas F., Jarvis K. S., and Gaffey M. J. (1994) Iron alteration minerals in the visible and near-infrared spectra of low-albedo asteroids. *Icarus, 109,* 274–283.

Vilas F., Cochran A. L., and Jarvis K. S. (2000) Vesta and the Vestoids: A new rock group? *Icarus, 147,* 119–128.

Wood J. H. and Kuiper G. P. (1963) Photometric studies of asteroids. *Astrophys. J., 137,* 1279–1285.

Xu S., Binzel R. P., Burbine T. H., and Bus S. J. (1995) Small Main-belt Asteroid Spectroscopic Survey: Initial results. *Icarus, 115,* 1–35.

Yamada M., Sasaki S., Nagahara H., Fujiwara A., Hasegawa S., Yano H., Hiroi T., Ohashi H., and Otake H. (1999) Simulation of space weathering of planet-forming materials: Nanosecond pulse laser irradiation and proton implantation on olivine and pyroxene samples. *Earth Planets Space, 51,* 1255–1265.

Zellner B., Tholen D. J., and Tedesco E. F. (1985) The eight-color asteroid survey: Results for 589 minor planets. *Icarus, 61,* 355–416.